ISSN 1814-4225 (print)
ISSN 2663-2012 (online)

UDC 533.63,534.23

doi: 10.32620/aktt.2024.6.03

Petro LUKIANOV

National Technical University of Ukraine "Igor Sikorsky Kyiv Polytechnic Institute", Kyiv, Ukraine

NUMERICAL–ANALITICAL METHOD FOR THE PROBLEMS OF AERODYNAMIC NOISE GENERATIONS IN HELICOPTER AND QUADROTORS

***The subject of this** paper is to demonstrate the capabilities of numerical-analytical method for solving problems of sound generation by helicopter and quadrocopter rotors. In particular, the finite difference schemes for the implementation of the numerical-analytical method for steady, non-steady 2-D potential flows describing the generation of noise of aerodynamic origin by a helicopter rotor blade are presented. Examples of the application of the numerical-analytical method to the problems of sound generation by a 3-D unsteady potential flow for the aerodynamic noise of a quadrotor are presented. It should be noted that until recently there was no unified finite difference scheme for solving helicopter rotor acoustics problems for different levels of physical approximations. The numerical-analytical method developed by the author of this paper has been shown to be capable of solving the problems of helicopter and quadrotor blade aeroacoustics for both simplified potential and significantly non-potential flows. **The research methods are based on** numerical schemes for the aerodynamic near and far sound fields calculations. The paper gives examples of the solution of these problems, analyses the application of the numerical-analytical method and compares it with existing finite difference methods. In particular, the calculation templates of the method for a stationary 2-D flow and a transient 3-D flow are presented and the special features of the selection of the number of points in the calculation template are explained. Depending on the specifics of a particular problem, the number of calculation templates and points in the calculation mesh can vary. This makes it possible to set up a stable calculation for each of the problems to be solved using the numerical-analytical method. In this case, the convergence of the method occurs automatically each time based on the idea of the numerical-analytical method itself. **Results and conclusions.** The results of a comparative analysis of existing numerical methods for calculating the sound field of helicopter and quadrocopter rotors have shown that the numerical-analytical method developed in detail is effective both for the calculation of sound formation problems in the potential approximation based on the Karman-Guderley equation and for the full system of sound generation equations based on the Navier-Stokes equation for the case of non-potential flow. The efficiency of the numerical-analytical method consists in the fact that it is implicit and allows to adjust the numerical scheme for each specific problem to be solved.*

***Keywords**: aerodynamic noise of helicopter and quadrotor rotors; numerical-analytical method.*

Introduction

The diversity of problems in aeroacoustics leads researchers to search for optimal numerical methods and schemes suitable for solving the problems of sound generation by flow for the widest possible class of problems. Before analysing the numerical methods, it is necessary to clarify the following: What is the difference between the process of sound generation and the process of sound radiation? The choice of numerical schemes and methods depends on the type of sound generation considered for a particular problem. Aeroacoustics studies the problems of sound generation, while classical acoustics studies sound radiation. The models and equations of aeroacoustics and the classical theory of sound radiation are different. This is because the process of sound generation in aeroacoustics has a different physical nature than in the classical theory of sound radiation. When a solid body vibrates with a small amplitude, it generates small disturbances in the air that propagate into the environment as a sound wave - this is sound radiation, i.e. classical acoustics. However, when a stream of air flows around a solid body, certain areas of flow instability occur during this flow, causing the occurrence of small sound disturbances within the flow itself, where the sound is generated directly in the flow itself - this is the process of sound generation governed by the equations of aeroacoustics. This explains the most important physical difference between sound generation and radiation. Both processes, radiation and generation, have been demonstrated in experimental studies of helicopter rotors, aeroplane propellers and quadcopters. There is still no general model that can describe both processes simultaneously. As a rule, these two physical processes are analysed mathematically separately: Physical models are created and equations are written down for each of them. This paper focuses on the difficulties encountered when applying numerical methods and schemes to solve the problems of helicopter and quadrotor aeroacoustics.

The instability of the flow resulting from the interaction of the blade with the airflow is reflected in the instability of the solutions of the equations and systems of equations describing the sound generation process. Therefore, numerical methods and design schemes should be able to take into account the areas of flow instability, as these areas are a source of intense noise generation. However, not every finite difference method is able to do this. Therefore, it is useful to emphasise those numerical schemes and methods that can numerically calculate the regions of physical instability of flows.

The investigation of noise of aerodynamic origin is an important task in the improvement of modern rotorcraft, especially helicopters and quadrocopters. In order to successfully solve the problem of reducing aerodynamic noise, it is necessary to find out which of the existing numerical methods are suitable for calculating a specific type of flow in which aerodynamic noise is generated. This paper focuses on a comparative analysis of existing numerical methods and a description of a numerical-analytical method for solving problems of the generation of noise of aerodynamic origin by the rotor of a helicopter or quadrotor. Examples of the application of the numerical-analytical method to solve specific problems of noise generation are given. The study of noise of aerodynamic origin is an important task in the process of improving modern rotorcraft, especially helicopters and quadrocopters. In order to successfully solve the problem of reducing noise of aerodynamic origin, it is necessary to find out which of the existing numerical methods are suitable for calculating a particular type of flow in which aerodynamic noise is generated. This paper focuses on a comparative analysis of existing numerical methods and a description of a numerical-analytical method for solving problems of the generation of noise of aerodynamic origin by the rotor of a helicopter or quadrotor. Examples of the application of the numerical-analytical method to solve specific problems of sound production are given.

It should be noted that the first attempts to study noise of aerodynamic origin were made using simple theoretical models, the aim of which was to determine the dependence of rotational noise on rotor kinematics and blade geometry. However, the range of topics was then considerably expanded once it was established that noise of aerodynamic origin has various components: Rotational noise, high-speed impulsive noise and noise from the interaction between vortices and blades. The mathematical models and equations that describe this or that type of noise differ. Accordingly, the methods of numerical calculation also differ, e.g. for rotational noise and blade-vortex interaction noise (BVI noise). The more complex the physical model and the equations with which it is mathematically implemented, the more noise sources it contains. Therefore, we will analyse the main existing models and numerical approaches used to describe different types of noise of aerodynamic origin from helicopter and quadrotor rotors.

1. Analysis of design schemes for sound generation by potential flow

The first type of noise investigated was helicopter rotational noise. A successful theoretical model for the study of rotational noise was proposed by Gutin [1]. This model clearly states that the rotational noise depends on the generated harmonics and the blade size. However, this model is only one-dimensional and does not provide any information about the type of noise generated directly in the environment.

The next step in the study of noise of aerodynamic origin is, as a potential approximation, to model the generation and propagation of small disturbances from a thin blade, which is governed by the Karman-Guderley (K-G) equation [2, 3]:

$$(K-(\gamma+1)\phi_x)\phi_{xx}+\phi_{yy}=0\,, \qquad (1)$$

where $K=(1-M_\infty^2)\delta^{2/3}$ is the transonic similarity parameter, $\gamma=c_p/c_V$ is the ratio of specific heat capacity.

At the beginning of research, this equation was only considered as an equation for small aerodynamic disturbances. Later, this model was considerably improved by many authors [4]. The complete three-dimensional unsteady equation for the generation of small sound disturbances was established in [5], where it was proved that the three-dimensional analogue of equation (1) is nothing but the equation for the generation of sound by a thin wing in the potential unsteady approximation.

Since equation (1) is a nonlinear differential equation, the boundary value problems based on it require a numerical solution. Let us consider the existing numerical methods for solving the two-dimensional steady-state and transient equation (1) and its three-dimensional transient analogue from [5] and analyse them.

It is known that equation (1), depending on the values of its parameters, allows the simultaneous existence of flow regions with subsonic and supersonic velocities in the flow. For this reason, it was not easy to choose a calculation scheme for the numerical solution of the problem based on the K-G equation.

ISSN 1814-4225 (print)
ISSN 2663-2012 (online)

The first successful attempt to solve the K-G equation numerically was the Murman-Cole scheme [6]. For the numerical implementation of the scheme, the authors write the equation (1) in a conservative form, which allows the use of a fully conservative scheme:

$$\left(\frac{w^2}{2}\right)_x - v_{\bar{y}} = 0\,, \tag{2}$$

where $w = \varphi_x = (\gamma+1)\phi_x - K$, $v = \varphi_{\bar{y}} = (\gamma+1)\phi_{\bar{y}}$.

Let (x, y) be any element with a uniform spacing of the difference grid in the plane (x, y), and the vertices have indices (i, j). Equation (2) can be written in conservative form for a cell centered on a point (i, j) (Fig. 1). This results in the following equation:

$$\left[\left(\frac{w^2}{2}\right)_{i+1/2,j} - \left(\frac{w^2}{2}\right)_{i-1/2,j}\right]\Delta\bar{y} - (v_{i,j+1/2} - v_{i,j-1/2})\Delta x = 0\,. \tag{3}$$

Otherwise, equation (3) can be written as:

$$\frac{1}{2}(w_{i+1/2,j} - w_{i-1/2,j})(w_{i+1/2,j} + w_{i-1/2,j})\Delta\bar{y} - \\ -(v_{i,j+1/2} - v_{i,j-1/2})\Delta x = 0\,. \tag{4}$$

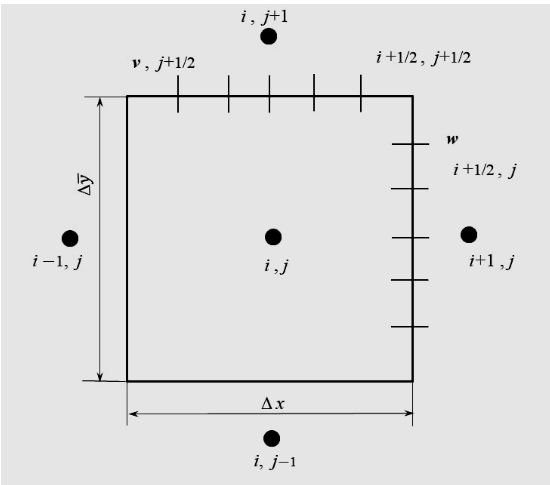

Fig. 1. Control cell

Now, if we solve an equation in a domain where it is an elliptic equation, i.e. a Laplace-type equation, then central finite differences are used to approximate both w and v:

$$v_{i,j+1/2} \equiv (\varphi_{\bar{y}})_{i,j+1/2} = \frac{\varphi_{i,j+1} - \varphi_{i,j}}{\vartriangle\bar{y}},\ v_{i,j-1/2} = \frac{\varphi_{i,j} - \varphi_{i,j-1}}{\vartriangle\bar{y}} \tag{5}$$

$$w^c_{i,j+1/2} \equiv (\varphi_x)_{i+1/2,j} = \frac{\varphi_{i+1,j} - \varphi_{i,j}}{\vartriangle\bar{y}},\ w_{i,j-1/2} = \frac{\varphi_{i,j} - \varphi_{i,j-1}}{\vartriangle\bar{y}} \tag{6}$$

Otherwise, equation (4) can be written as:

$$\left(\frac{\varphi_{i+1,j} - \varphi_{i-1,j}}{2\vartriangle x}\right)\left(\frac{\varphi_{i+1,j} - 2\varphi_{i,j} + \varphi_{i-1,j}}{(\vartriangle x)^2}\right) - \\ -\left(\frac{\varphi_{i,j+1} - 2\varphi_{i,j} + \varphi_{i,j-1}}{(\vartriangle\bar{y})^2}\right) = 0\,. \tag{7}$$

Equation (7) is a second-order central difference scheme, which is an approximation of the equation for the elliptic (subsonic) domain. The stability of this scheme, the fulfillment of the Courant-Friedrichs-Levy criterion, is described in detail in the monograph of one of the authors of this scheme [4].

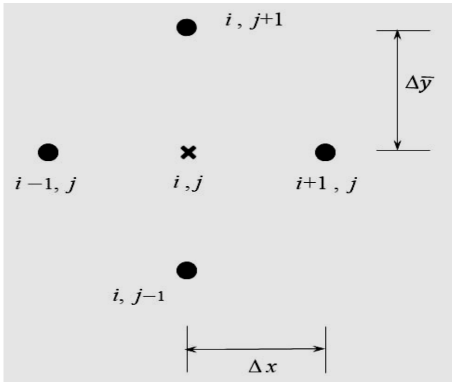

Fig. 2. The calculation pattern in the elliptical domain

This pattern is not suitable for the hyperbolic (sonic) flow region because it contains upstream points. To avoid such influence, the computational template for the first (nonlinear) term of Eq. 2, which is responsible for the formation of shock waves that are converted into sound waves, is shifted downstream by one point at index i + 1 → I (Fig.3):

$$\left(\frac{\varphi_{i,j} - \varphi_{i-2,j}}{2\vartriangle x}\right)\left(\frac{\varphi_{i,j} - 2\varphi_{i-1,j} + \varphi_{i-2,j}}{(\vartriangle x)^2}\right) - \\ -\left(\frac{\varphi_{i,j+1} - 2\varphi_{i,j} + \varphi_{i,j-1}}{(\vartriangle\bar{y})^2}\right) = 0 \tag{8}$$

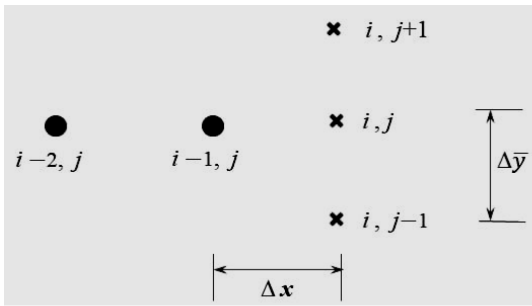

Fig. 3. Calculation pattern in the hyperbolic area

What happens in the region of the sound points where the flow is accelerated or decelerated to the speed of sound? In this region of the flow, a different pattern is proposed, which does not match either the hyperbolic or the elliptical pattern (Fig.4):

$$\left(\frac{\varphi_{i+1,j}-\varphi_{i,j}+\varphi_{i-1,j}+\varphi_{i-2,j}}{2\triangle x}\right)\times$$
$$\times\left(\frac{\varphi_{i+1,j}-\varphi_{i,j}+\varphi_{i-1,j}+\varphi_{i-2,j}}{(\triangle x)^2}\right)- \qquad (9)$$
$$-\left(\frac{\varphi_{i,j+1}-2\varphi_{i,j}+\varphi_{i,j-1}}{(\triangle \bar{y})^2}\right)=0.$$

As you can see from the example of the solution to the problem described above, it is not possible to get by with just one numerical template for different flow regions. The finite difference scheme considered above is a first order accuracy scheme in the hyperbolic flow domain [6]. In the elliptic flow domain, this scheme has a second order accuracy.

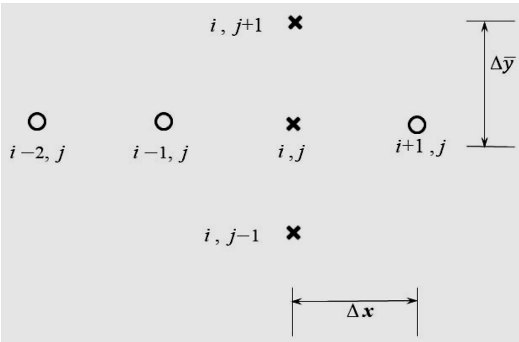

Fig. 4. Calculated operator pattern at one point of the shock wave

The second-order accuracy difference schemes for the hyperbolic domain are given in [6], and the methods to derive them are discussed in the monograph [7]. An analysis of the coupled compression jumps, which significantly affect the use of numerical schemes, was carried out in [8]. Later works using this calculation method appeared [9], but for the equation in full potentials, without separating small perturbations from the flow. In [9] a plane unsteady flow was calculated. For the mixed time and coordinate derivatives, both the central and the mixed finite differences were used. The second time derivative is modelled by backward finite differences. All this allowed us to simulate the pressure shock on the shock wave to a certain degree.

So far we have not discussed which flow properties are of interest when investigating a shock wave. To analyse the solution of the K-equation, which describes the propagation of small disturbances on a thin wing, the pressure coefficient C_p is of interest. It is defined as the ratio $C_p = 2(p-p_\infty)/\rho_\infty U^2$. The numerical methods mentioned above calculate the pressure coefficient in the form of a parabola when there is no shock wave in the flow. If there is a discontinuity in the pressure curve, i.e. a shock wave is realised, the profile looks like a deformed, ‘broken’ parabola [4] (Fig. 5):

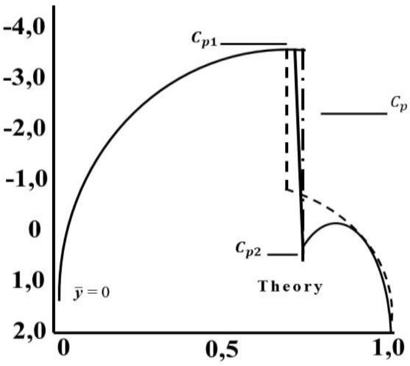

Fig. 5. Pressure distribution for k = 1.8

It should be noted that the pressure coefficient for the propagation of small disturbances in an unsteady flow deviates significantly from the parabolic form, as experience from later studies on unsteady plane transonic flow has shown. This discrepancy can be explained by the fact that the numerical schemes actually considered do not take into account the instability of the flow: In them, the shock wave is as if it were stopped with respect to time. Therefore, it makes sense to further consider the schemes for solving the unsteady case of the K-G equation.

In the second half of the 70s of the last century, some authors resorted to an implicit calculation scheme with variable directions - ADI (alternating direction implicit) - to solve the plane unsteady problem for the equation of propagation of small disturbances on a thin wing. In [10], for example, this method is used for the case of a low-frequency unsteady two-dimensional flow. In this case, the K-G equation is solved in the following form:

$$A\phi_{tt}+2B\phi_{xt}=C\phi_{xx}+\phi_{yy}\,, \qquad (10)$$

where

$$A=k^2M_\infty^2/\delta^{2/3}, B=kM_\infty^2/\delta^{2/3},$$
$$C=(1-M_\infty^2)/\delta^{2/3}-(\gamma+1)M_\infty^m\phi_x\,.$$

In this expression, the parameter m is the function M_∞. The parameter is a fitting parameter for the critical value of the pressure coefficient [11]. The time parameter $k=\omega c/U_\infty$ is the Strouhal number. The coordinates

 ISSN 1814-4225 (print)
ISSN 2663-2012 (online)

x, y in (10) were used as a running coordinates:

– at the coordinate x:

$$2B(\Delta t)^{-1}\delta_x(\bar{\phi}^{n+1}_{j,k} - \phi^n_{j,k}) = D_x f_{j,k} + \delta_{yy}\phi^n_{j,k}; \quad (11)$$

– at the coordinate y:

$$2B(\Delta t)^{-1}\delta_x(\phi^{n+1}_{j,k} - \bar{\phi}^n_{j,k}) = \frac{1}{2}\delta_{yy}(\phi^{n+1}_{j,k} - \phi^n_{j,k}), B = \\ = kM^2_\infty / \delta^{2/3}, \quad (12)$$

$$\delta_x\phi_{j,k} = 2(\phi_{j,k} - \phi_{j-1,k})(x_{j+1} - x_{j-1})^{-1} = \\ = (3\phi_{j,k} - 4\phi_{j-1,k} + \phi_{j-2,k})(x_{j+1} - x_{j-1})^{-1}, \quad (13)$$

$$\delta_{yy}\phi_{j,k} = 2[(\phi_{j,k+1} - \phi_{j,k})(y_{k+1} - y_{k-1})^{-1} - \\ -(\phi_{j,k} - \phi_{j,k-1})(y_k - y_{k-1})^{-1}](y_{k+1} - y_{k-1})^{-1}, \quad (14)$$

$$f_{j,k} = \frac{1}{2}[C^n_{j,k}\phi^{n+1}_{x_j,k} + (1 - M^2_\infty)\phi^n_{x_j,k} / \delta^{2/3}], \quad (15)$$

$$\phi_{x_{j+1/2},k} = (\phi_{x_{j+1},k} - \phi_{x_j,k})(x_{j+1} - x_{j-1}), \quad (16)$$

$$Df_{j,k} = 2(x_{j+1} - x_{j-1})^{-1}[(1-\varepsilon_j)\times \\ \times(f_{j+1/2,k} - f_{j-1/2,k}) + \\ + \varepsilon_{j-1}(f_{j-1/2,k} - f_{j-3/2,k})], \quad (17)$$

here

$$\varepsilon_j = 0, \text{ if } C^n_{j+1/2,k} + C^n_{j-1/2,k} > 0;$$

$$\varepsilon_j = 1, \text{ if } C^n_{j+1/2,k} + C^n_{j-1/2,k} < 0.$$

Following this work, there are further publications that improve the methodology for modelling the flow at a compression jump (shock wave). In [12, 13], for example, the method of jump separation and stretching of the grid coordinates is used. Shock waves are considered as discontinuities perpendicular to the flow direction. Somewhat later [14], the authors develop their approach for three-dimensional flows, but not for the K-G equation, but for the full streaming potential equation. In the early 1980s, the paper [15] was published, which solved the inverse problem: the flow field and the shape of the airfoil are determined from a given pressure.

However, the variety of numerical schemes for the different cases of the K-H equation makes it inconvenient to solve the problems in general: It would be desirable to use a general numerical scheme that would solve the problem for each case of the K-H equation. This method was proposed by the author in 2005 [16] for simplified cases of the K-G equation and later developed for the full three-dimensional K-G equation. As it turned out later, the numerical-analytical method easily coped with the case of sound generation by non-potential flow. Below you will find a diagram of the numerical-analytical method for solving the K-G equation and for the complete system of aeroacoustic equations for a non-potential flow.

2. Numerical analytical method

The numerical analytical method [17, 18] has been successfully tested on a series of solved problems of noise generation by a helicopter blade. The basic idea of the method is that the finite difference representation of the derivatives is not explicitly used in the equations to be solved. The reason for this is simple: it is not always known in advance which of the expansions will be the most stable during the calculation. According to the idea of the numerical-analytical method, we proceed as follows: At the $n-1$ points of the computational ‘template’ we perform a standard expansion into a multidimensional Taylor series, and at the point we assume that the equation of small perturbation propagation is automatically satisfied. In fact, we require that the equation for the generation of small transient K-G perturbations is satisfied at the n-th point. Under this condition, the convergence condition of the desired numerical solution is automatically satisfied. In this case, the coefficients of the Taylor series expansion are implicitly expressed from the system of equations. This scheme of the method is used for certain boundary value problems where the boundary condition allows integration. Therefore, the boundary condition is not added to the system of equations. However, this is only done in simple cases.

If it is also necessary to satisfy a constraint, which is the case for most problems, the constraint is added to the equation system of the calculation. In this case we have the following: at the $n-2$ points of the calculation ‘template, we perform a multidimensional Taylor series expansion and require the automatic execution of the equation to be solved and the boundary condition. This reduces the number of points in the design scheme for which a Taylor series expansion is required by 2.

In the following, we consider the implementation of the numerical-analytical method for the two-dimensional stationary and three-dimensional unsteady K-G equation.

2.1. The 2-dimensional case

The Karman-Guderley equation (1) in dimensionless variables $\xi = x/c, \eta = \lambda y$ has the form:

$$[1 - \frac{1}{M^2} + \varepsilon\cdot(\gamma+1)f_\xi]f_{\xi\xi} - \frac{\lambda^2}{M_1^2}f_{\eta\eta} = 0. \quad (18)$$

A 6-point scheme was proposed for the two-dimensional case [17] (Fig. 6):

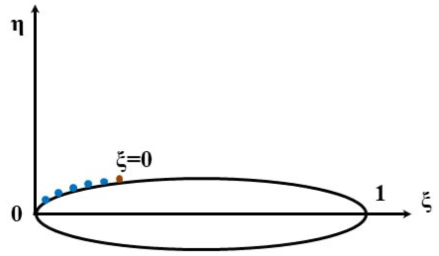

Fig. 6. Calculated points of the 6-point pattern

we expand the function at five points $f(\xi_i, \eta_i)$ in Taylor's series ($f \in C^2([0;1]\times[0;1])$):

$$\begin{aligned}
&f(\xi_i, \eta_i) = f(\xi_0, \eta_0) + f_\xi(\xi_0, \eta_0)(\xi_i - \xi_0) + \\
&+ f_\eta(\xi_0, \eta_0)(\eta_i - \eta_0) + \\
&+ \frac{1}{2}[f_{\xi\xi}(\xi_0, \eta_0)(\xi_i - \xi_0)^2 + \\
&+ 2f_{\xi\eta}(\xi_0, \eta_0)(\xi_i - \xi_0)(\eta_i - \eta_0) + \\
&+ 2f_{\eta\eta}(\xi_0, \eta_0)(\eta_i - \eta_0)^2] + \\
&+ o(\max\{(\xi_i - \xi_0)^2, (\eta_i - \eta_0)^2, (\xi_i - \xi_0)(\eta_i - \eta_0)\}), \\
&(i = 1, \ldots, 5). \qquad (19)
\end{aligned}$$

At the 6th calculation point (ξ_0, η_0), we require the equation to be executed automatically:

$$\begin{aligned}
&[1 - \frac{1}{M^2} + \varepsilon \cdot (\gamma + 1) f_\xi(\xi_0, \eta_0)] f_{\xi\xi}(\xi_0, \eta_0) - \\
&- \frac{\lambda^2}{M_1^2} f_{\eta\eta}(\xi_0, \eta_0) = 0.
\end{aligned} \qquad (20)$$

The boundary condition that there is no flow

$$f_\eta = \delta g_\xi, 0 < \xi < 1 \qquad (21)$$

is automatically satisfied in this problem. The system of 6 equations (19), (20) thus enables us to find all unknown derivatives of the dimensionless sound potential $f(\xi_i, \eta_i)$ and the potential itself. It is not difficult to see how simple the idea of the numerical-analytical method is, but at the same time, as further calculations have shown, the method is very practical.

The scheme of the numerical method described above enabled the direct fulfillment of the convergence condition of the method, and the implicit nature of the scheme, the choice of the required number of Taylor series terms, ensured the stability of the calculation. The curves of pressure coefficients at Mach numbers $M \approx 1$ presented in Fig.7 and Fig.8 show that the numerical-analytical method successfully coped with the task of calculating the sound flow in a physically unstable region (Fig. 8). At the same time, the numerical scheme has not "collapsed", as is the case with most known finite difference representations.

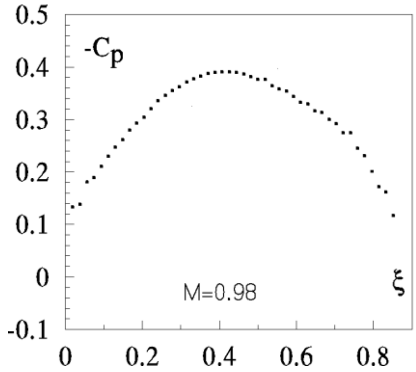

Fig. 7. Calculation of the pressure coefficient in the transonic flow area

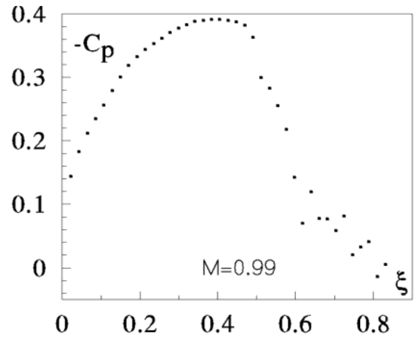

Fig. 8. Calculation of the pressure coefficient in the transonic flow area

2.2. The 3-dimensional case

The author of this paper has previously derived the full three-dimensional equation for the propagation of small perturbations on a thin wing [5] and performed a theoretical analysis of special cases. The numerical-analytical method has also been used to solve the boundary value problem in the study of the generation and propagation of small unsteady disturbances from a helicopter blade. In this case, it is applied to a dimensionless 3-dimensional equation for the propagation of small disturbances $f(\xi_i, \eta_i, \zeta_i, \tau_i)$ from a thin blade:

$$\begin{aligned}
&\left(\frac{kc}{U}\right)^2 f_{\tau\tau} + [1 - \frac{1}{M_1^2} + (1+\gamma)\varepsilon f_\xi] f_{\xi\xi} + \frac{2kc}{U} f_{\xi\tau} - \\
&- \frac{(\lambda c)^2}{M_1^2} f_{\eta\eta} - \left(\frac{c}{R}\right)^2 \frac{1}{M_1^2} f_{\zeta\zeta} = 0, \qquad (22)
\end{aligned}$$

where $\xi = x/c, \eta = \lambda y, \zeta = z/R, \tau = kt$ - dimensionless coordinates and time.

ISSN 1814-4225 (print)
ISSN 2663-2012 (online)

Boundary conditions:

$$\delta\left[\frac{kc}{U}g_{\tau}+g_{\xi}\right]=\varepsilon\lambda cf_{\eta}, 0<\xi<1, \eta=\eta(\xi). \qquad (23)$$

Then, in analogy to the above example for the two-dimensional case, we choose the number of design points of the template according to the number of unknown derivatives in the function represented in the Taylor series expansion, but by 2 less, since we still have to solve the equation (22) and the boundary condition (23). In this case, the dimensionless potential can be written as:

$$\begin{aligned} f(\xi_i,\eta_i,\zeta_i,\tau_i) &= f(\xi_o,\eta_o,\zeta_o,\tau_o)+f_{\xi}(\xi_i-\xi_o)+ \\ &+f_{\eta}(\eta_i-\eta_o)+f_{\zeta}(\zeta_i-\zeta_o)+f_{\tau}(\tau_i-\tau_o)+ \\ &+\frac{1}{2}[f_{\xi\xi}(\xi_i-\xi_o)^2+f_{\eta\eta}(\eta_i-\eta_o)^2+f_{\zeta\zeta}(\zeta_i-\zeta_o)^2+ \\ &+f_{\tau\tau}(\tau_i-\tau_o)^2]+f_{\xi\eta}(\xi_i-\xi_o)(\eta_i-\eta_o)+ \\ &+f_{\xi\zeta}(\xi_i-\xi_o)(\zeta_i-\zeta_o)+f_{\eta\zeta}(\zeta_i-\zeta_o)(\eta_i-\eta_o)+ \\ &+f_{\xi\tau}(\xi_i-\xi_o)(\tau_i-\tau_o)+f_{\eta\tau}(\eta_i-\eta_o)(\tau_i-\tau_o)+ \\ &+f_{\zeta\tau}(\zeta_i-\zeta_o)(\tau_i-\tau_o)+R(\Delta^3), i=1,n-2, \qquad (24) \end{aligned}$$

here $R(\Delta^3)$ is a residual term of Taylor's series.

For the three-dimensional transient case, we thus have $n=15$. During the numerical calculation, the time step was adjusted according to the Courant-Friedrichs-Levy criterion [19]: During a dimensionless time step, the sound wave was located in a cell in space. This condition made it possible to perform a physically correct and stable calculation that takes into account the physical properties of the sound wave. Fig.9 shows the calculation of the pressure coefficient at the blade cross-section. Since the pressure coefficient is a function of only small sound disturbances (see [5]), it obviously describes the zones of local sound generation near the blade surface. As can be seen from the figure, the pressure distribution according to the transient model differs significantly from the pressure distribution according to the steady-state model (Fig. 9): The profile C_p no longer looks like a parabola, as observed for a flat steady-state problem, but has the shape of a short-time impulse signal with local maxima, indicating the possible existence of a series of shock waves [18].

Recently, the problem of reducing energy consumption and noise in small civil aviation has become more and more acute. The use of air cabs is one way to solve this problem. The author of this paper has calculated the rotor noise of a quadrotor air cab using a potential model [20]. A 15-point scheme of the numerical-analytical method was used for the numerical calculation.

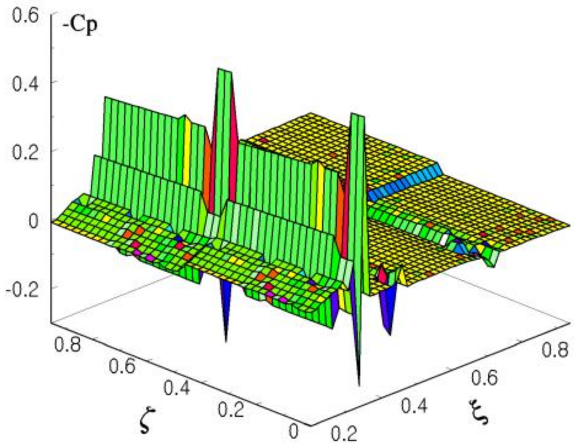

Fig. 9. Pressure coefficient on the surface of the helicopter blade

The comparison of Fig. 10 and Fig. 11 shows that the distribution of the pressure coefficient in the area of the main fault is similar to a certain extent to Fig. 9. Nevertheless, there are certain differences in each calculation case. The obtained calculation data in the three-dimensional approximation clearly show the existence of areas with intense sound generation, as described in detail in [20].

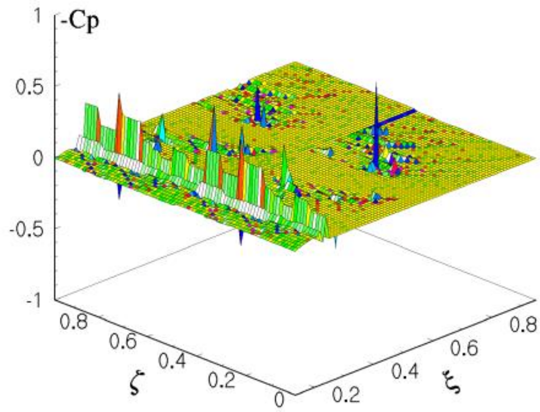

Fig. 10. Pressure coefficient on the surface of the quadcopter blade

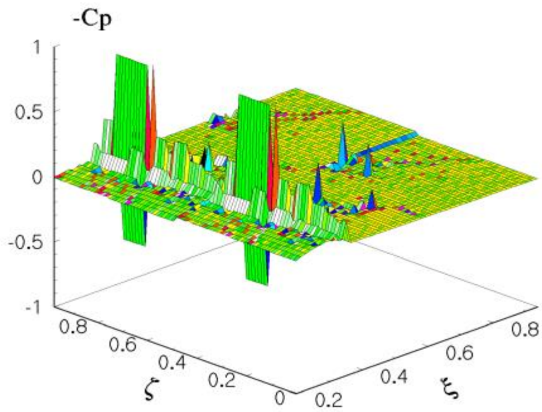

Fig. 11. Pressure coefficient on the surface of the quadcopter blade

3. Construction scheme of the non-potential flow

The existing schemes for calculating sound disturbances in the potential approach have been discussed above. Potential models are typically used in modelling blade noise for relatively high Mach numbers M>0.5, when rotational noise rather than vortex noise dominates. At M<0.5, the vortex component of the flow contributes significantly to the overall noise level, so that the potential approximation is no longer physically correct. In this case, equations or systems of equations that take into account the vortex component of the flow are used to model the noise generation of aerodynamic origin.

Currently, a sufficient number of non-potential models [21, 22] are known to describe the generation of sound of aerodynamic origin. However, the best known models from this list are not physically accurate. In particular, when choosing a model to calculate helicopter noise, most researchers are guided by the most popular models Ffowc's Willams-Hawkins (FW-H) [23] and Farassat's 1A [24]. In some cases, Lighthill's acoustic analogy is also used [25]. However, this does not mean that the above models are physically correct: Lighthill's acoustic analogy and its application within the FW-H formula leaves open the question of the physical correctness of these approaches [26].

Let us consider the Ffowcs Willams-Hawkins equation:

$$4\pi^2(\rho-\rho_0)=\frac{\partial^2}{\partial x_i \partial x_j}\int\limits_{V_0}[\frac{T_{ij}}{r|1-M_r|}]d\eta-\frac{\partial}{\partial x_i}\int\limits_{S}[\frac{p_{ij}n_j}{r|1-M_r|}]dS(\eta)-$$

$$-\frac{\partial^2}{\partial x_i}\int\limits_{V_0}[\frac{\rho_0 v_i}{r|1-M_r|}]d\eta+\frac{\partial^2}{\partial x_i \partial x_j}\int\limits_{V_0}[\frac{\rho_0 v_i v_j}{r|1-M_r|}]d\eta\ . \qquad (25)$$

It is easy to see that equation (25) contains the Lighthill equation. However, in [25] Lighthill has obtained his own equation artificially: by adding a certain term (derivative) on the left and right sides, which formally gives it the appearance of a wave equation that seems to describe the generation of sound. The question arises: what kind of equation do we get if we add more derivatives on the left and right sides of the equation? This question implies that the approach used by Lighthill is not physically correct, because if we add and subtract certain derivatives to the equation without explanation, we actually get equations that describe a completely different physical process. How can we be sure that this is the equation of sound generation? Adding or subtracting does not help: if you take away these added terms, i.e. perform the same mathematical transformation in the opposite direction, the resulting equation is no longer a wave equation.

The added term on the right-hand side of the Lighthill equation actually introduced non-existent sound sources. On the other hand, if, for example, there is an equation of motion in terms of forces, then adding or subtracting a particular term will result in a change in the physical process, i.e. it will be an equation describing a different physical process (with different forces) than before the addition or subtraction of that term. The mathematical technique used by Lighthill is therefore physically incorrect. Since the Ffowcs-Willams-Hawkins formula is derived directly from Lighthill's equation, the question of its physical correctness also arises.

According to the formula derived by Farassat [24], the sound pressure is determined by a thickness source $p_T^{'}(x,t)$ and a load source $p_L^{'}(x,t)$:

$$4\pi p^{'}(x,t)=4\pi(p_T^{'}(x,t)+p_L^{'}(x,t))=\frac{\partial}{\partial t}\int\limits_{f=0}[\frac{\rho_0 v_n}{r(1-M_r)}+$$

$$+\frac{p\cos\theta}{cr(1-M_r)}]_{ret}dS+\int\limits_{f=0}[\frac{p\cos\theta}{r^2(1-M_r)}]_{ret}dS\,, \qquad (26)$$

where $\cos\theta=n_i\hat{r}_i$ is the local angle between the normal to the surface and the radiation direction.

If you take a close look at equations (25) and (26), you will realise that these approaches say nothing about the determination of the near sound field. The methods for determining the sound field potential or the density in the sound wave is not mentioned either. However, these physical variables in the sound wave must be known and taken into account when calculating the far-field integrals.

The main drawback of Farassat's approach is that the sound sources are non-existent fictitious sources located inside a solid surface, a blade. And we are talking about sound of aerodynamic origin, i.e. that which is generated inside the air flow, and not in a solid body, where in principle it cannot occur. The question arises: why is such a strange approach used? The answer is simple: In classical acoustics, the Green's function in the form of a point source is used as an auxiliary solution (not as the main solution!) to represent the far sound field. This makes it possible to write down the specified representation of the far sound field for real sound sources in a mathematically correct way on the basis of Green's second formula. Farassat went even further: he assumed that it did not necessarily have to be real sound sources, but that it could also be imaginary sources. And these sources are located within a rigid surface that emits no sound at all. And this is precisely the main obstacle to the physical determination of aerodynami-

ISSN 1814-4225 (print)
ISSN 2663-2012 (online)

cally generated sound: with this approach, there are no real sound sources at all. There are no real sound sources that can be included in the wave equation, only fictitious sources that appear to be contained in a rigid surface. But these fictitious sources do not actually produce any sound at all. This has been discussed in Fedorchenko's work [26] as well as in [5]. Can such a model be considered physically correct? No, of course not.

It is worth mentioning that new numerical schemes explaining the solution of aeroacoustic problems have appeared recently, e.g. [27, 28] and [29], but in reality the authors numerically model complete systems of aerodynamic-thermodynamic equations, trying to study the noise of jets. The aeroacoustic equations of Lighthill, Ffowc's Willams-Hawkins and Farassat are not mentioned at all. In these works, attention is drawn to the issue of the absence of dispersion in numerical schemes and non-reflection conditions are established [29]. The problem of asynchrony of the time step [27] in a numerical scheme is most likely to be considered when the speed of sound wave propagation is variable, i.e. depends essentially on changes in thermodynamic parameters. This is possible in the case of a non-isentropic flow. In this case, the speed of the sound wave and thus the Courant number is different in each calculation cell. For jet engines, the isentropic condition is not fulfilled. This can justify the use of different cell sizes for the time variable. In the case of an isentropic flow, whose model is sufficiently valid to describe the noise generation of helicopter and quadrotor propellers, the speed of sound can be approximated as a constant value, since thermodynamic changes are neglected. In this case, there is no need for an asynchronous time step of the calculation grid.

In addition to the models mentioned above, there are a number of other models that describe sound of aerodynamic origin [26], but each of these models has certain physical limitations. The most complete physically correct theoretical model was previously proposed by the author of this paper [30]. The closed-form system of equations obtained based on this model in the case of isentropic flow is as follows:

$$\frac{\partial^2\bar\rho'}{\partial\tau^2}-\frac{1}{M_\infty^2}\frac{\partial^2\bar\rho'}{\partial\xi^2}-a^2\left(\lambda^2c^2\cdot\frac{\partial^2\bar\rho'}{\partial\eta^2}+\frac{1}{AR^2}\cdot\frac{\partial^2\bar\rho'}{\partial\zeta^2}\right)+$$
$$+R\left(\bar\rho',\frac{\partial\bar\rho'}{\partial\xi},\frac{\partial\bar\rho'}{\partial\eta},\frac{\partial^2\bar\rho'}{\partial\xi^2},\frac{\partial^2\bar\rho'}{\partial\eta^2},\frac{\partial^2\bar\rho'}{\partial\xi^2},\frac{\partial^2\bar\rho'}{\partial\xi\partial\eta},...,\frac{\partial^2\bar\rho'}{\partial\zeta^2}\right)=$$
$$=\gamma\left(\bar\rho',\frac{\partial\bar\rho'}{\partial\xi},\frac{\partial\bar\rho'}{\partial\eta},\frac{\partial^2\bar\rho'}{\partial\xi^2},\frac{\partial^2\bar\rho'}{\partial\eta^2},\frac{\partial^2\bar\rho'}{\partial\xi^2},\frac{\partial^2\bar\rho'}{\partial\xi\partial\eta},...,\frac{\partial^2\bar\rho'}{\partial\zeta^2}\right), \tag{27}$$

$$\bar\rho\left(\frac{\partial^2\bar\varphi}{\partial\xi^2}+\lambda^2c^2\frac{\partial^2\bar\varphi}{\partial\eta^2}+\frac{1}{AR^2}\frac{\partial^2\bar\varphi}{\partial\zeta^2}\right)+c\frac{\partial\bar\rho}{\partial\xi}\frac{\partial\bar\varphi}{\partial\xi}+\lambda^2c^2\frac{\partial\bar\rho}{\partial\eta}\frac{\partial\bar\varphi}{\partial\eta}+$$
$$+\frac{1}{AR^2}\frac{\partial\bar\rho}{\partial\zeta}\frac{\partial\bar\varphi}{\partial\zeta}=-[c\frac{\partial\bar\rho}{\partial\tau}++\bar\rho'\left(c\frac{\partial\bar u}{\partial\xi}+\lambda c^2\frac{\partial\bar v}{\partial\eta}+\frac{c^2}{R}\frac{\partial\bar w}{\partial\zeta}\right)+$$
$$+c\bar u\frac{\partial\bar\rho'}{\partial\xi}+\lambda c^2\bar v\frac{\partial\bar\rho'}{\partial\eta}+\frac{c^2}{R}\bar w\frac{\partial\bar\rho'}{\partial\zeta}], \tag{28}$$

here $\bar\varphi,\bar\rho'$ – are dimensionless sound potential and density; $\bar\rho,\bar u,\bar v,\bar w$ – are the dimensionless density and components of the velocity vector of the main flow.

$$R\left(\bar\rho',\frac{\partial\bar\rho'}{\partial\xi},\frac{\partial\bar\rho'}{\partial\eta},\frac{\partial^2\bar\rho'}{\partial\xi^2},\frac{\partial^2\bar\rho'}{\partial\eta^2},\frac{\partial^2\bar\rho'}{\partial\xi^2},\frac{\partial^2\bar\rho'}{\partial\xi\partial\eta},...,\frac{\partial^2\bar\rho'}{\partial\zeta^2}\right)$$

contains all terms of the right-hand side (28) that depend on the sound density and its derivatives. The right-hand side of Eq.(28) contains only the terms that depend on the derivatives of the dimensionless sound potential:

$$\gamma\left(\bar\rho',\frac{\partial\bar\rho'}{\partial\xi},\frac{\partial\bar\rho'}{\partial\eta},\frac{\partial^2\bar\rho'}{\partial\xi^2},\frac{\partial^2\bar\rho'}{\partial\eta^2},\frac{\partial^2\bar\rho'}{\partial\xi^2},\frac{\partial^2\bar\rho'}{\partial\xi\partial\eta},...,\frac{\partial^2\bar\rho'}{\partial\zeta^2}\right).$$

The system of differential equations (27), (28) allows us to describe the process of sound generation with second order accuracy and is physically correct, since its derivation is based on the classical Rayleigh approach [31, 32] to determine the wave equation.

4. Examples of the application of the numerical-analytical method in the case of non-potential flows

4.1. Noise generation during the landing of a helicopter

Despite the mathematical complexity of the system of equations (27), (28), the author has succeeded in numerically solving a number of interesting problems using the numerical-analytical method [33, 34]. The special feature of the numerical-analytical method is the use of a non-uniform computational grid around the blade. For example, when solving the problem of noise generation by a double-curvature blade (Fig. 12 and Fig. 13), the grid spacing along the blade chord was about twice as small as that along the blade span and varied within $[\xi\times\zeta]=[82\times40]$. Such a difference in grid size had no influence on the detection of the transient effects shown in Fig. 12 and Fig. 13. However, the different step size along the spatial coordinates allowed us to save computer resources. The data obtained from the calculation of the near-field using the numerical-analytical method were used to calculate the integral representation of the far-field.

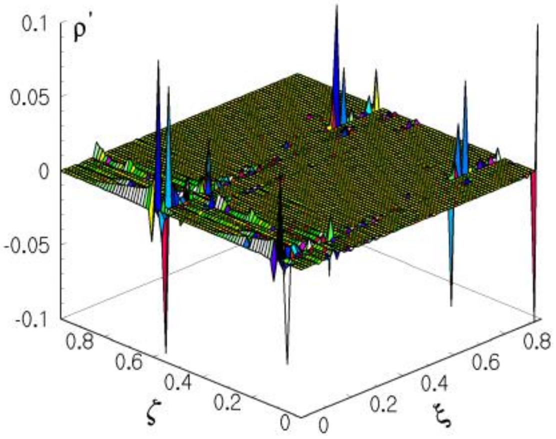

Fig. 12. Acoustic density distribution over the surface of a helicopter blade

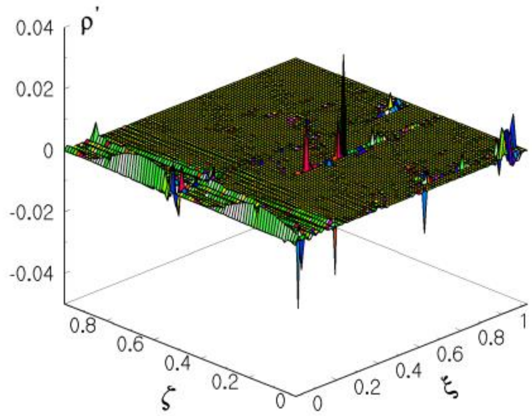

Fig. 13. Acoustic density distribution over the surface of a helicopter blade

4.2. Vortex Ring Mode

One of the interesting problems solved by the numerical-analytical method is the problem of generating the noise of the helicopter-rotor interaction in the “vortex ring” mode of operation [35]. A 15-point scheme was also used in the numerical implementation of the method. The computational grid contained nodes. The peculiarity of the numerical-analytical method made it possible to “capture" local inhomogeneity in the behavior of acoustic density fluctuations, Fig.14 and Fig.15. The general picture of these fluctuations helps us to identify areas of intense sound generation when we change the parameters of the problem and the blade geometry. This is very useful for finding optimal aerodynamic and acoustically quiet blade shapes.

By recording the change in acoustic characteristics with external sensors and comparing it with the obtained graphical dependencies, it is possible to diagnose the helicopter's entry into the “vortex ring”, which allows the pilot to react in time and remove the helicopter from this mode to prevent a catastrophe. A more detailed description of the solution to this problem can be found in [35].

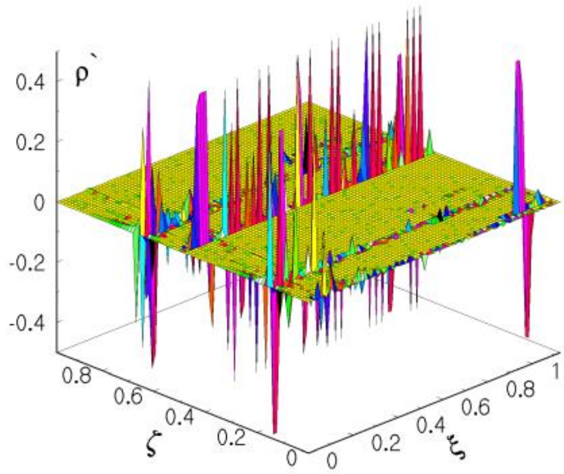

Fig. 14. Acoustic density distribution over the surface of a helicopter blade in “vortex ring” mode

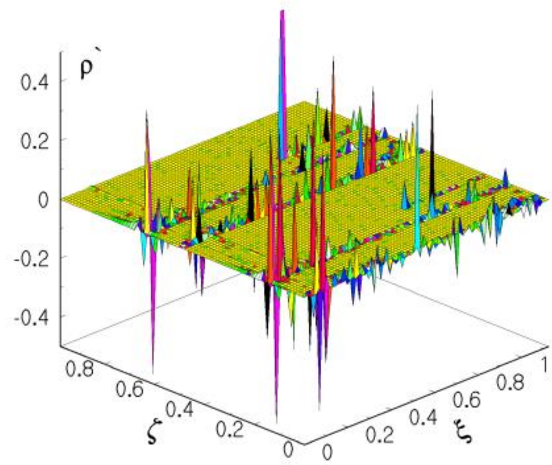

Fig. 15. Acoustic density distribution over the surface of a helicopter blade in “vortex ring” mode

Discussion

The results of a comparative analysis of numerical methods for solving problems of noise generation of aerodynamic origin of helicopter and quadrotor rotors have shown that the numerical-analytical method is an effective tool for this class of problems. In particular, the numerical-analytical method can be used for both two-dimensional stationary and three-dimensional nonstationary noise generation problems. This is an essential feature of the method compared to other numerical schemes that are used exclusively for specific computational cases. In addition, the constructed scheme of the method is simple and constructive, so that the calculation template can be easily customised for each specific problem.

ISSN 1814-4225 (print)
ISSN 2663-2012 (online)

Conclusions

1. In this paper, we analyses numerical methods to calculate the near-sonic field for the cases of potential and non-potential flow of helicopter and quadrotor rotors.

2. The analysis has shown that until recently there was no single finite difference scheme or method for different flow models of sound generation. This problem was solved using the numerical-analytical method.

3. The special feature of the numerical-analytical method is that it is an implicit finite-difference representation that makes it possible to calculate the properties of both the sound field fluctuations and the main flow field itself on a control design surface near a body that interacts with the flow and generates sound during this interaction. The calculated data is also used in the integral representation previously proposed by the author. This generally allows the calculation time of the noise to be significantly reduced, as no calculation on a three-dimensional volume is required.

4. The ability of the numerical-analytical method to solve the problems of helicopter noise generation for both potential and non-potential flows allows us to consider this method, to a certain extent, universal for various problems of noise generation of aerodynamic origin by rotors.

Conflict of Interest

The author declare that they have no conflict of interest in relation to this research, whether financial, personal, authorship or otherwise, that could affect the research and its results presented in this paper.

Financing

The research was conducted without financial support.

Data availability

The work has no associated data.

Use of Artificial Intelligence

The author confirms that he did not use artificial intelligence methods while creating the presented work.

References

1. Gutin, L. Y. On sound field of a rotating propeller. *NASATM-1195*, 1948, pp. 1-22. Available at: https://ntrs.nasa.gov/citations/20030068996. (accessed 10.08.2024).

2. Karman, T. von. The similarity low of transonic flow. *Journal of Math. and Phisics*, 1947, vol. 26, iss. 3, pp. 182-190. Available at: https://www.semanticscholar.org/paper/The-Similarity-Law-of-Transonic-Flow-K%C3%A1rm%C3%A1n/32f50657d5bca4a5663fb18cc90808b0d0e732da. (accessed 10.08.2024).

3. Guderley, G.Considerations of the Structure of Mixed Subsonic and Supersonic Flow Patterns. *Wright Field Report*, F-TR-2168- ND,October,1947.

4. Cole, J. D., Cook, L. P. Transonic Aerodynamics. *Elsevier*, 2012. 482 p. Available at: https://books.google.com.ua/books/about/Transonic_Aerodynamics.html?id=3n7bBmzdBH8C&redir_esc=y. (accessed 10.08.2024).

5. Lukianov, P. V. Nestatsionarnoye rasprostraneniye malykh vozmushcheniy ot tonkogo kryla: blizhneye i dal'neye pole [Unsteady propagation of small disturbances from a thin wing: The near and a far fields]. *Acoustic bulletin*, 2009, vol. 12, no. 3, pp. 41-55. Available at: https://hydromech.org.ua/content/pdf/av/av-12-3(41-55).pdf. (accessed 10.08.2024). (In Russian).

6. Murman, E. M. Calculation of Plane Steady Transonic Flows. *AIAA Journal*, 1971, vol. 9, no.1, pp. 114-121. DOI: https://doi.org/10.2514/3.6131.

7. Hirsch, Ch. *Numerical computetion of Internal and External Flows. Vol. 1. Fundamentals of Computational Fluid Dynamics*, Second Edition. Elsevier, Burlington, USA, 2007. 675 p.

8. Murman, E. M. Analysis of Embeded Shock Waves Calculated by Relaxation Methods. *AIAA Journal*, 1974, vol. 12, iss. 5, pp. 626-633. DOI: https://doi.org/10.2514/3.49309.

9. Caradonna, F. X., & Isom, M. P. Subsonic and Transonic Potential Flow over Helicopter Rotor Blades. *AIAA Journal*, 1972, vol. 10, iss. 12, pp. 1606-1612. DOI: https://doi.org/10.2514/3.50404.

10. Ballhaus, W. R., & Goorjian, P. M. Implicit finite-Difference Computations of Unsteady Transonic Flows about Airfoils Including the Effect of Irregular Shock Motions. *AIAA Journal*, 1977, vol. 15, iss. 12, pp. 1728-1735. DOI: https://doi.org/10.2514/3.60838.

11. Ballhaus, W. F. Some Recent Progress in Transonic Flow Computations,VKL Lecture Series:Computational Fluid Dynamics. *Von Karman Institute for Fluid Dynamics*, Rhode-SAt-Genese, Belgium, March 15-19, 1976. Available at: https://ntrs.nasa.gov/citations/19790010775. (accessed 10.08.2024).

12. Yu, N. J., Seebass, A. R., &Ballhaus, W. F. Implicit Shock-Fitting Scheme for Unsteady Transonic Flow Computations. *AIAA Journal*, 1978, vol. 16, iss. 7, pp. 673-678. DOI: https://doi.org/10.2514/3.60957.

13. Fung, K.-Y., Yu, N. J., & Seebass, A. R. Small Unsteady Perturbations in Transonic Flows. *AIAA Journal*, 1978, vol. 16, iss. 8, pp. 815-822. DOI: https://doi.org/10.2514/3.60968.

14. Sobieczky, H. Yu. New Method for Designing Shock-Free Transonic Configurations. *AIAA Journal*, 1979, vol. 17, iss. 7, pp. 722-729. DOI: https://doi.org/10.2514/3.61209.

15. Fung, K.-Y., & Chung, A. W. Computations of unsteady transonic aerodynamics using prescribed steady pressures. *Journal of Aircraft*, 1983, vol. 20, iss.

12, pp. 1058-1061. DOI: https://doi.org/10.2514/3.48212.

16. Lukianov, P. V. Primeneniye chislenno-analiticheskogo metoda dlya resheniya zadach akustiki [Using of numerical-analytical method for acoustic problems solution]. *Acoustical symposium* "*Consonanse 2005"*, Kiev-2005, Inst. Hydromechanics, 27-29 September, pp. 225-230. Available at: https://hydromech.org.ua/content/pdf/cons/cons2005_225-230.pdf. (accessed 10.08.2024). (In Russian).

17. Lukianov, P. V. Pro odyn chyselno-analitychnyi pidkhid do rozviazannia zadachi heneratsii zvuku tonkym krylom. Chastyna I. Zahalna skhema zastosuvannia dlia ploskoi statsio-narnoi zadachi. [On one numerically-analytical approach to solving of a problem on sound generation by a thin wing. Part I. General schematic of application to planer stationary problem]. *Akustychnyj visnyk - Acoustic bulletin*, 2011, vol. 14, iss. 3, pp. 46-52. Available at: http://hydromech.org.ua/content/uk/av/av-14-3.html. (accessed 10.08.2024). (In Russian).

18. Lukianov, P. V. Ob odnom chislenno-analiticheskom podhode k resheniju zadachi generacii zvuka tonkim krylom. Chast' II. Shema prilozhenija k nestacionarnym zadacham [On one numerical-analytical approach to solving of a problem on sound generation by a thin wing. Part II. A schematic of application to non-stationaty problems]. *Akustychnyj visnyk - Acoustic bulletin*, 2012, vol. 15, iss. 3, pp. 45-52. Available at: http://hydromech.org.ua/content/ru/av/15-3_45-52.html. (accessed 10.08.2024). (In Russian).

19. Courant, R., Friedrichs, K., & Lewy, H. Uber die partiellen Differenzengleichungen der mathematischen Physik. *Mathematische Annalen*, 1928, vol. 100, pp. 32-74. Available at: https://www.semanticscholar.org/paper/%C3%9Cber-die-partiellen-Differenzengleichungen-der-Courant-Friedrichs/c63f1868620752ecb4d8c47a86631a25649fe6b4. (accessed 10.08.2024).

20. Lukianov, P., & Dusheba, O. Modeling of Aerodynamic Noise of Quadrotor Type Aerotaxis. *Aerospace technic and technology*, 2023, vol. 4, pp. 38-49. DOI: https://doi.org/10.32620/aktt.2023.4.05.

21. Lukianov, P. V. Generatsiya zvuka tonkim trekhmernym krylom: dal'neye pole [System of aeroacoustic equations for the medium with vorticity: general case]. *Acoustical symposium* "*Consonanse 2007"*, Kiev-2007, Inst. Hydromechanics, 25-27 September, pp. 163-168. Available at: https://hydromech.org.ua/content/pdf/cons/cons2007-157-162.pdf. (accessed 10.08.2024). (In Russian).

22. Lukianov, P. V. Ob odnoy modeli aeroaxustiki vyazkogo sjimaemogo gaza. Chast I. Analiz suschestvuyuschih modeley, vyivod razreshayuschey sistemyi uravneniy [On one model for aeroacousics of viscous compressible gas. Part I Analysis of existing models, dedusing of resolving system of equations]. *Acoustic bulletin*, 2013-2014, vol. 16, iss. 2, pp. 18-30. Available at: https://hydromech.org.ua/content/pdf/av/av-16-2(18-30).pdf. (accessed 10.08.2024). (In Russian).

23. Willams, F. J. E., & Hawkings, D. L. Sound Generated by Turbulence and Surfaces in Aritrary Motion. *Philosophical Transactions of the Royal Socicety A*, 1969, vol. 264, iss. 1151, pp. 321-342. DOI: https://doi.org/10.1098/rsta.1969.0031.

24. Farassat, F. Derivation of Formulations 1 and 1A of Farassat. *NASA/TM*, 2007-214853, March-2007, 25 p. Available at: https://ntrs.nasa.gov/citations/20070010579. (accessed 10.08.2024).

25. Lighthill, M. J. On sound Generated Aerodynamically I. Genaral Theory. *Proceedings of the Royal Society A*, 1952, vol. 211, iss. 1107, pp. 564-587. DOI: https://doi.org/10.1098/rspa.1952.0060.

26. Fedorchenko, A. T. On some fundamental flaws in present aeroacoustic theory. *Journal of Sound and Vibration*, 2000, vol. 232, iss. 4, pp. 719-782. DOI: https://doi.org/10.1006/jsvi.1999.2767.

27. Semiletov, V. A., & Karabasov, S. A. Cabaret scheme for computational aeroacoustics:extension to asynchronous time stepping and 3D flow modeling. *Int. Journ. Aeroacoustics*, 2014, vol. 13, iss. 3-4, pp. 321-336. DOI: https://doi.org/10.1260/1475-472X.13.3-4.321.

28. Markesteijn, A. P., & Karabasov, S. A. Time asynchronous relative dimension in space method for multi-scale problems in fluiad dynamics. *Journal of Compuatational Physics*, 2014, vol. 258, iss. 1, pp. 137-164. DOI: https://doi.org/10.1016/j.jcp.2013.10.035.

29. Tam, C. K. W., & Webb, J. C. Dispertion-Relation-Preserving Finite Difference Schemes for Computational Acoustics. *Journal of Computational Physics*, 1993, vol. 107, iss. 2, pp. 262-281. DOI: https://doi.org/10.1006/jcph.1993.1142

30. Lukianov, P. V. Ob odnoy modeli aeroakustiki vyazkogo szhimayemogo gaza. Chast' II. Shum blizkogo vzaimodeystviya vikhrya i lopasti vertoleta [On one model for aeroacousics of viscous compressible gas. Part II Noise of near helicopter blade-vortex interaction noise]. *Acoustic bulletin*, 2013-2014, vol. 16, iss. 3, pp. 31-40. Available at: https://hydromech.org.ua/content/pdf/av/av-16-3(31-40).pdf. (accessed 10.08.2024). (In Russian).

31. Rayleigh, J. W. S. *The theory of sound. Vol. 1.* Dover Publications, 1945. 520 p. Available at: https://books.google.com.ua/books/about/The_Theory_of_Sound.html?id=v4NSAlsTwnQC&redir_esc=y. (accessed 10.08.2024).

32. Rayleigh, J. W. S. *The theory of sound. Vol. 2.* Dover Publications, 1945. 522 p. Available at: https://books.google.com.ua/books/about/The_Theory_of_Sound.html?id=Frvgu1wSFfUC&redir_esc=y. (accessed 10.08.2024).

33. Lukianov, P. V. Snizheniye BVI-shuma rotora vertolota s pomoshch'yu lopasti s dvoynym izgibom [Helicopter's rotor BVI-noise reduction by twice-bent blade]. *Bulletin of Cherkassy University*, *Ser.: Mathematics, Informatics*, 2017, no. 1-2, pp. 50-64. Available at: http://www.irbis-nbuv.gov.ua/cgi-bin/irbis_nbuv/cgiirbis_64.exe?I21DBN=LINK&P21DBN=UJRN&Z21ID=&S21REF=10&S21CNR=20&S21STN

ISSN 1814-4225 (print)
ISSN 2663-2012 (online)

=1&S21FMT=ASP_meta&C21COM=S&2_S21P03=FILA=&2_S21STR=VchuM_2017_1-2_7. (accessed 10.08.2024). (In Russian).

34. Lukianov, P. V. Osobennosti generatsii BVI-shuma pri samolotnoy posadke vertolota [The pecularities of BVI-noise generation at helicopter airplane landing]. *Bulletin of Zaporozhsky National University. Ser.: Phys. and Math. Sciences*, 2018, no. 2, pp. 73-88. DOI: https://web.znu.edu.ua/cms/index.php?action=category/browse&site_id=5&lang=ukr&category_id=1340&path=ves-arkhiv/2018/1333/1340&category_code=1340 (In Russian).

35. Lukianov, P. V. Osoblyvosti heneratsiyi BVI-shumu rotora helikoptera na rezhymi «Vykhrove kil′tse» [Pecularities of generation of BVI-noise of a helicopter rotor in ”Vortex ring” mode]. *Computer Science and Applied Mathematics*, 2021, iss. 2, pp. 36-44. DOI: https://doi.org/10.26661/2413-6549-2021-2-04. (in Ukrainian).

Надійшла до редакції 15.10.2024, прийнята до опублікування 20.11.2024

ЧИСЕЛЬНО-АНАЛІТИЧНИЙ МЕТОД ДЛЯ ЗАДАЧ ГЕНЕРАЦІЇ АЕРОДИНАМІЧНИХ ШУМІВ РОТОРАМИ ГЕЛІКОПТЕРІВ ТА КВАДРОКОПТЕРІВ

П. В. Лук'янов

Предметом даної роботи є демонстрація можливостей чисельно-аналітичного методу для розв'язання задач генерації звуку роторами гелікоптерів та квадрокоптерів. Зокрема, наведено скінченно-різницеві схеми для реалізації чисельно-аналітичного методу для стаціонарних та нестаціонарних двовимірних потенціальних течій, що описують генерацію шуму аеродинамічного походження лопаттю ротора гелікоптера. Наведено приклади застосування чисельно-аналітичного методу до задач генерації звуку нестаціонарною тривимірною потенційною течією для аеродинамічного шуму квадрокоптера. Слід зазначити, що до недавніх пір не існувало єдиної скінченно-різницевої схеми розв'язання задач акустики ротора гелікоптера для моделей різних фізичних рівнів наближень. Показано, що чисельно-аналітичний метод, розроблений автором даної роботи, дозволяє розв'язувати задачі аероакустики лопаті гелікоптера та квадрокоптера як для спрощених потенціальних, так і для суттєво непотенціальних течій. **Методи дослідження грунтуються** на чисельних схемах розрахунку аеродинамічних ближнього і дальнього звукового поля. У статті наведено приклади розв'язання цих задач, проаналізовано застосування чисельно-аналітичного методу та проведено його порівняння з існуючими методами скінченних різниць. Зокрема, наведено розрахункові шаблони методу для стаціонарної 2-вимірної течії та перехідної 3-вимірної течії і пояснено особливості вибору кількості точок у розрахунковому шаблоні. Залежно від специфіки конкретної задачі кількість розрахункових шаблонів і точок в розрахунковій сітці може змінюватися. Це дає можливість налаштувати стабільний розрахунок для кожної з задач, що розв'язуються чисельно-аналітичним методом. При цьому збіжність методу відбувається щоразу автоматично, виходячи з ідеї самого чисельно-аналітичного методу. **Результати та висновки**. Результати порівняльного аналізу існуючих чисельних методів розрахунку звукового поля роторів вертольотів і квадрокоптерів показали, що детально розроблений чисельно-аналітичний метод є ефективним як для розрахунку задач звукоутворення в потенційному наближенні на основі рівняння Кармана-Гудерлі, так і для повної системи рівнянь звукоутворення на основі рівняння Нав'є-Стокса для випадку непотенційної течії. Ефективність чисельно-аналітичного методу полягає в тому, що він є неявним і дозволяє адаптувати чисельну схему до кожної конкретної задачі, яка розв'язується.

Ключові слова: аеродинамічний шум роторів вертольотів і квадрокоптерів; чисельно-аналітичний метод.

Лук'янов Петро Володимирович – канд. фіз.-мат. наук, старш. наук. співроб., доц. каф. авіа- та ракетобудування, Національний технічний університет України «КПІ ім.Ігоря Сікорського», Київ, Україна.

Petro Lukianov – Candidate of Physics and Mathematics Sciences, Senior Researcher, Associate Professor of the Department of Avia- and rocket constructions, National Technical University of Ukraine “KPI named after Igor Sikorsky”, Kyiv, Ukraine,
e-mail: p.lukianov@kpi.ua, ORCID: 0000-0002-7584-1491.